DOI 10.1007/s11182-015-0563-0

Russian Physics Journal, Vol. 58, No. 6, October, 2015 (Russian Original No. 6, June, 2015)

STRUCTURE AND HARDNESS OF 01570 ALUMINUM ALLOY FRICTION STIR WELDS PROCESSED UNDER DIFFERENT CONDITIONS

R. R. Il'yasov,[1] E. V. Avtokratova,[1] M. V. Markushev,[1] P. Yu. Predko,[2] and V. Yu. Konkevich[2]

UDC 538.91

Structure and hardness of the 01570 aluminum alloy joints processed by friction stir welding at various speeds are investigated. It is shown that increasing the traverse tool speed lowers the probability of macrodefect formation in the nugget zone; however, this can lead to anomalous grain growth in the zone of contact with the tool shoulder. Typical "onion-like" structure of the weld consisting of rings that differ by optical contrast is formed for all examined welding regimes. It is demonstrated that this contrast is caused by the difference in the grain sizes in the rings rather than by their chemical or phase composition. Mechanisms of transformation of the alloy structure during friction stir welding are discussed.

Keywords: aluminum alloy, friction stir welding, microstructure, microhardness.

INTRODUCTION

The process of friction stir welding (FSW) that has been developed relatively recently [1– 3] is a highly effective method of solid-state joining of metals and alloys, including aluminum-based alloys, as demonstrated by the existing practice of its industrial application [4, 5]. Despite active investigations performed in many countries, the nature of structurization during FSW is still unclear in many respects. Meanwhile, the knowledge of mechanisms and regularities of the structural and phase transformations of materials being joined as a function of their initial state and welding parameters is important and is in fact necessary for a clear understanding of the essence of the process, its effective application, and further development.

The aim of the present work is to investigate the influence of FSW regimes of 01570 aluminum alloy sheets of the Al–Mg–Sc–Zr system on the microstructure and hardness of the welds.

MATERIAL AND METHODS OF RESEARCH

Hot-rolled sheets of the 01570 aluminum alloy (with composition, in wt.%: Al –5.91Mg – 0.42 Mn – 0.24 Sc – 0.1 Zr) were welded with different tool traverse speeds (and constant tool rotation rate) at the Special Design Bureau "Salyut." Qualitative and quantitative analysis of the alloy structure in the joints was performed in the traverse plane by the standard methods of optical metallography (OM) and scanning and transmission electron microscopy (SEM and TEM, respectively). The macro- and microstucture was examined for specimens etched in Keller's reagent using a Nikon L150 optical microscope. The dislocation structure was investigated using a JEOL-2000EX transmission electron microscope. An electron backscattered diffraction (EBSD) analysis was carried out using a TESCAN MIRA 3

[1]Institute for Metals Superplasticity Problems of the Russian Academy of Sciences, Ufa, Russia, e-mail: ilyasov@imsp.ru; avtokratova@imsp.ru; mvmark@imsp.ru; [2]MATI – Russian State Technological University Named after K. É. Tsiolkovsky, Moscow Russia, e-mail: konkevich@mail.ru. Translated from Izvestiya Vysshikh Uchebnykh Zavedenii, Fizika, No. 6, pp. 16–20, June, 2015. Original article submitted March 6, 2015.

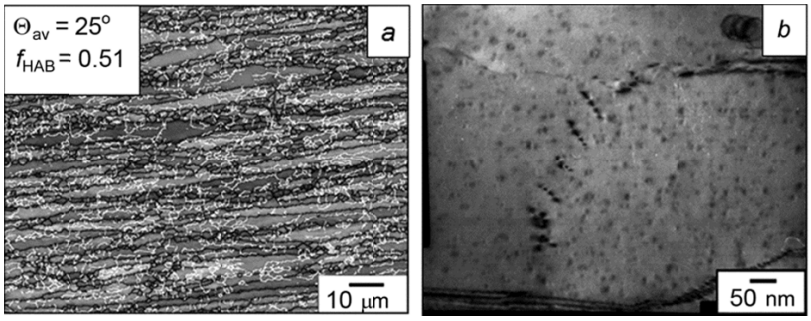

Fig. 1. Microstructure of the alloy 01570 in the initial sheet: *a*) SEM-EBSD image and *b*) TEM image.

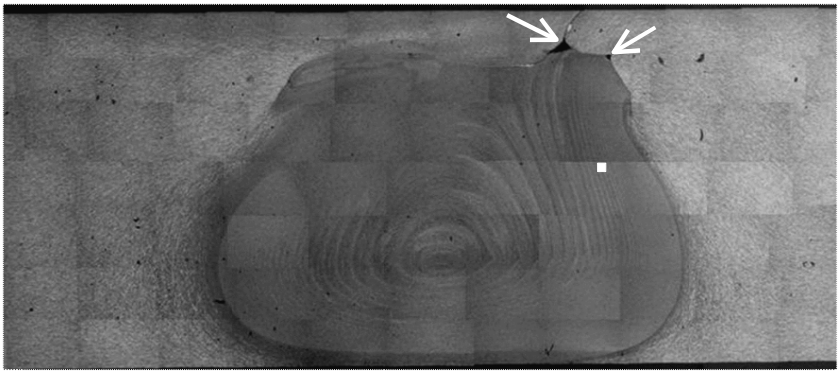

Fig. 2. Macrostructure of the FSW sheet joints processed with low tool traverse speed. The arrows indicate defects of the weld, and the square shows the region depicted in Fig. 3*a*.

LMH scanning electron microscope and the software package *HKL Channel 5*. Low-angle (from 2 to 15°) boundaries in the images of the reconstructed structures were marked in white, and high-angle (greater than 15°) boundaries were marked in black. The objects for the TEM and SEM analyses were prepared by jet electropolishing using a TenuPol-5 apparatus. X-ray microanalysis (XMA) of particles and OM of zones with different etchability were performed using a TESCAN VEGA-3 LMU scanning electron microscope. The microhardness of the alloy was measured during 10 s using an Axiovert-100 optical microscope with an MHT-10 attachment (control unit) and a load of 0.5 N.

RESULTS AND DISCUSSION

The microstructure of the sheets outside the weld zone was mainly represented by coarse fibers having a thickness of a few micrometers and elongated in the rolling direction (Fig. 1*a*). Fine grains were observed along the fiber boundaries, and a grid of low-angle boundaries dividing the fibers into fragments (subgrains) were detected within the fiber bodies. The relative fraction of the high-angle boundaries f_{HAB} in the structure was close to 50%, and the average misorientation angle for all boundaries Θ_{av} was about 25° (Fig. 1*a*). High densities of nanodispersed phases – the secondary aluminides of transition metals Al_3(Sc, Zr) (dispersoids) being products of decomposition of the aluminum solid solution anomalously supersaturated by scandium and zirconium upon homogenization and subsequent hot deformation of the ingot (Fig. 1*b*) – were observed within the (sub)grain bodies and along the boundaries.

Analysis of the macrostructure of the welded joint obtained with slow tool traverse speed revealed in the upper part of the weld the presence of macrodefects in the form of gaps in the zone of contact of the welded sheets with the shoulder of the tool (Fig. 2). The microstructure of the weld itself, as a whole, was fine-grained and represented by alternating layers with different optical contrasts forming the so-called *onion ring* structure [2, 3]. A distinguishing

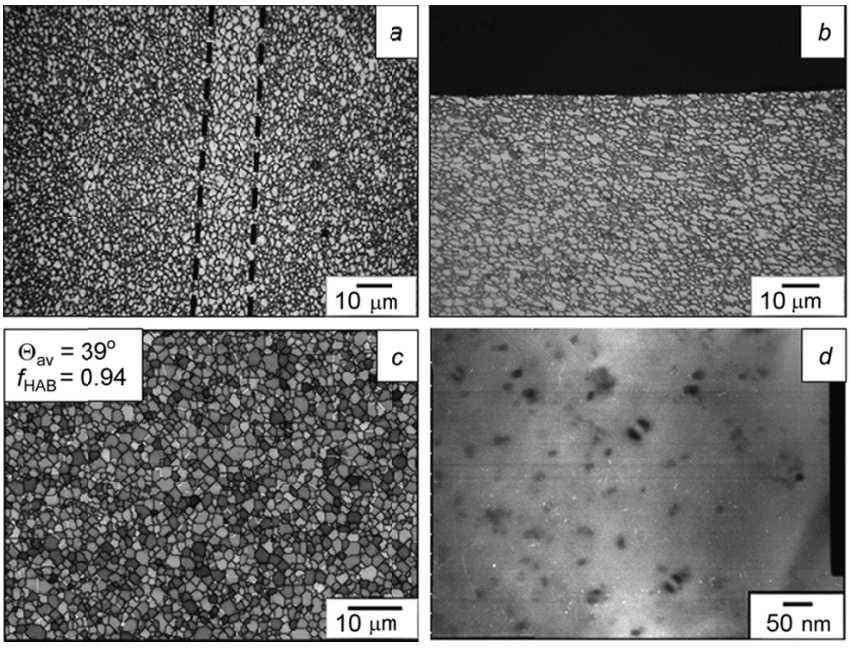

Fig. 3. Structure of the weld after FSW with low tool traverse speed: *a*) OM structure in the zone designated in Fig. 2 (the bright ring is marked off by the dashed line), *b*) zone of contact with the tool, *c*) EBSD map from the bright ring, and *d*) TEM image of dispersoids inside of the nugget zone.

feature of the structure of the upper part of the joint was a quite abrupt transition from the fibrous structure of the initial sheet to the uniaxial fine-grained structure of the weld. For the most part of the thermomechanically affected zone this transition occupied an extended region, giving the possibility to trace out the regularities of the transformation of the fibrous structure into the fine-grained one and to analyze the main mechanisms of the alloy grain refinement. Thus, at first the preferred spatial orientation of the fibers changed resulting in rotations of their axes, local bending, and fragmentation. Activation of these processes then led to the formation of the *S*-shaped (fir-tree) mixed structure in which the volume fraction of fine grains continuously increased when approaching to the nugget zone [6]. A completely recrystallized fine-grained structure having the average grain size of about 1 and 2 μm in the dark and bright rings, respectively, was observed in the core (Fig. 3*a*). Approximately the same grain size was observed in the zone of close contact with the tool shoulders (Fig. 3*b*).

The angular parameters of the microstructure varied in accordance with variation of the fine grain fraction in the structure of the joint. As a result, the fraction of high-angle boundaries in the core of the weld increased to $f_{HAB} = 0.94$, and the average misorientation angle of the boundaries reached ~40° (Fig. 3*c*). In the fine structure of the nugget zone, the lattice dislocation density was lower than in the thermomechanically affected zone. In this case, the dispersoids preserved their coherency within the matrix; however, their number was somewhat diminished, probably due to dissolution of small particles and growth of larger ones (Fig. 3*d*).

Results of x-ray microanalysis showed that the chemical composition in the core of the weld joint was identical in the neighbor rings and corresponded to the composition of the alloy, which was also observed in [7]. This suggests that the difference in the optical ring contrasts is not due to inhomogeneity of chemical composition of the matrix and/or distribution of particles of secondary phases caused by the specifics of the weld processing and its specific conditions, as was pointed out, for example, in [8]. It seems most likely that this contrast is due to different grain sizes in neighboring rings caused by peculiarities of the macroflow and formation of layers during FSW (traverse speed, deformation degree, etc.) as well as by the intensity of post-deformation grain growth. In turn, all above-indicated processes in this alloy are largely governed by the dispersoids and depend on their size and density. This was repeatedly pointed out in many studies, including [9] where the role of dispersoids and of their parameters for obtaining a stable

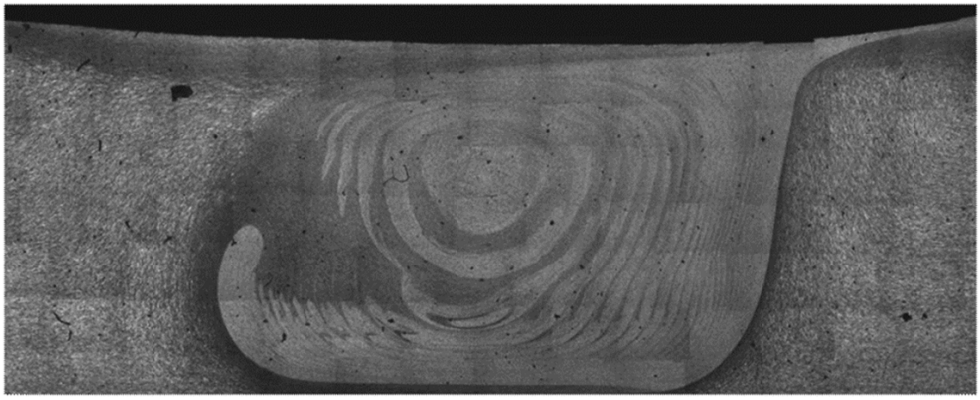

Fig. 4. Macrostructure of an FSW weld obtained with high tool traverse speed.

ultrafine-grained structure in the alloy 01570 of similar composition by equal-channel angular pressing was discussed. To answer the question which of the parameters has the predominant effect on the behavior of the alloy during FSW observed in the present study requires additional investigations. However, in our opinion, it is most likely that changes in the grain structure of the alloy were determined largely by the kinetics of grain growth during welding and the fraction of particles that lost coherency within the matrix. This is also confirmed by results of comparative analysis of the joint structure and hardness presented below.

An increase in the tool traverse speed led to a change in both the macro- and microstructure of the weld joint, expressed primary through a change in the shape of the weld core and in the absence of macrodefects in the form of gaps in the joint (Fig. 4). It should be noted that the *onion-like* character of the macrostructure was preserved; however, the thickness of the rings became noticeably larger, leading to the formation of a less dispersed and less homogeneous structure in the weld core and adjacent zones. Moreover, the grain size in the rings increased in the dark rings up to $d \approx 1.5$ μm and in the bright rings up to $d \approx 3$ μm (Fig. 5*a*). It should also be noted that, as in the previous case, a difference in the chemical composition of the rings could not be found.

A distinguishing feature of the weld structure is the fact that grains in the upper part of the joint grew to an anomalously large size $d \approx 10$ μm (Fig. 5*b*). In addition, our measurements revealed a large size of the (sub)grains (up to 3 μm) and a small fraction of high-angle boundaries ($f_{\text{HAB}} = 0.88$) in the core of the weld. Results of the TEM analysis, as in the previous case, revealed a low density of lattice dislocations indicating that the recovery and recrystallization of the structure proceeded to completion. In this case, the size of aluminides of transition metals was slightly higher (Fig. 5*d*). All this indicated that the maximum temperature in the center of the weld, in particular in the zone under the tool, was higher and caused the anomalous growth of grains even in such a complex alloy with large amounts of transition metals.

Thus, the data on the structure of FSW joints of the 01570 alloy demonstrate that dispersed precipitations of aluminides of transition metals play the dominant role in the formation of the weld structure, and their density and morphology determine the peculiarities of the weld structure.

The measured hardness of the examined joints also confirmed this conclusion. Judging from the data presented in Fig. 6, it is clear that the microhardness distribution and level across the axis of the joints depend directly on the FSW regime. Thus, after welding with a low tool traverse speed, the microhardness of the alloy varied insignificantly (Fig. 6). Only a weak diminution (by 5–8% in all) of its level in the core of the weld was noted. The reason for such behavior is probably the formation of a specific completely recrystallized ultrafine-grained structure and a crystallographic texture in the core as well as the detected coagulation of the dispersoids. With increasing tool traverse speed, the decrease of the alloy microhardness in the weld was more pronounced – a drop from 110 to 95 HV. In this case, when going through the boundary of the nugget zone of the weld core, an abrupt drop of the alloy hardness was noted. This was due to a more abrupt transition from the initial fibrous structure to the equiaxed fine-grained one. In addition to the decrease in the dispersoid size, a greater reduction of the alloy hardness in this case was apparently due to the large sizes of the recrystallized grains in the weld, expressing itself in a lower value of the Hall–Petch strengthening.

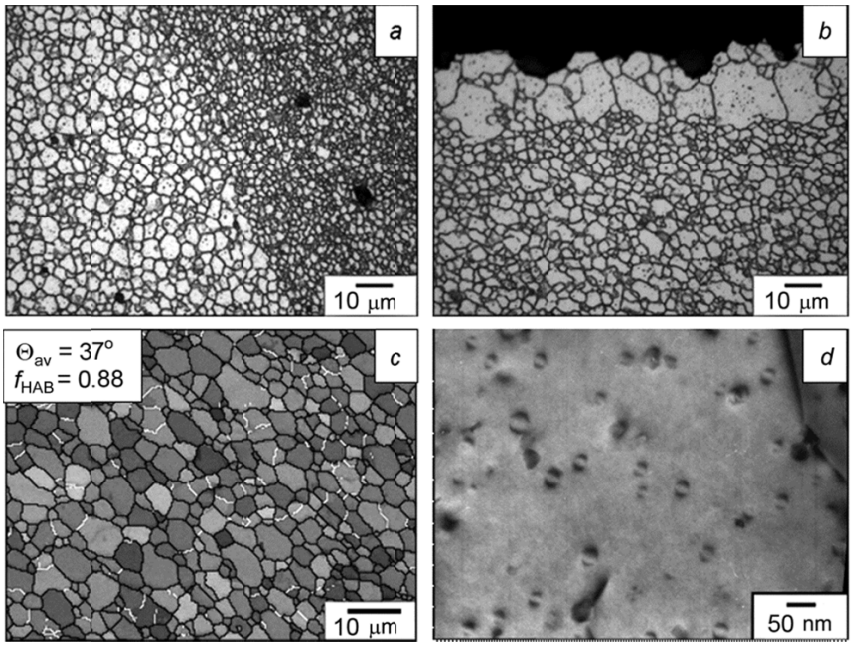

Fig. 5. Structure of an FSW joint obtained with high tool traverse speed: *a*) boundaries of the rings, *b*) zone of contact with the tool shoulder, *c*) EBSD pattern from a bright ring, and *d*) TEM image of the dispersoids.

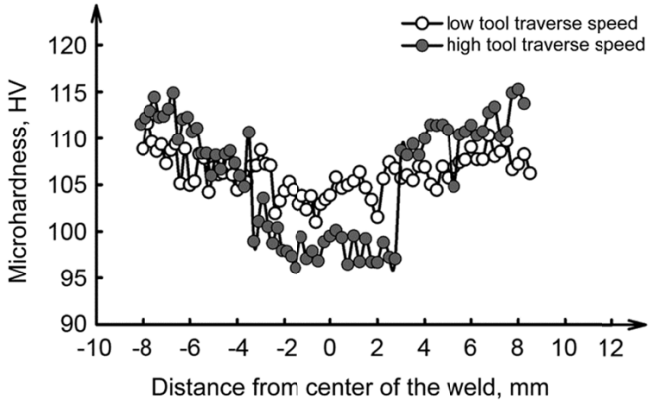

Fig. 6. Microhardness distribution in the weld zone after FSW with different tool traverse speeds.

CONCLUSIONS

1. During FSW of the 01570 alloy sheets, a banded (onion-like) fine-grained structure is formed in the core of the weld caused by the difference in grain sizes in the rings. This is not connected with a redistribution of the alloying elements.

2. Increasing the traverse tool rate leads to increased inhomogeneity of the structure and hardness distribution across the weld against the background of elimination of macrodefects in the form of gaps in the zone of contact with the tool.

3. The ultrafine-grained structure of the FSW joint is formed during continuous dynamic recrystallization directly in the process of interaction of the tool with the material being welded and is followed by the normal grain growth during cooling of the joint.

REFERENCES

1. W. M. Thomas, E. D. Nicholas, J. C. Needham, *et al*., The Welding Institute: TWI, PCT World Patent Application WO 93/10935, Field: 27 /November 1993 (UK 9125978.8, 6 December 1991), Publ: 10 June 1993.
2. R. S. Mishra and Z. Y. Ma, Mater. Sci. Eng., **R50**, 1–78 (2005).
3. N. G. Tret'yak, Avtomatich. Svarka, No. 7, 12–21 (2002).
4. A. Andersson, A. Norlin, and J. Backlund, Adventure Technology and Process, Stuttgart, Germany (1997).
5. O. Midling, in: Proc, 7th Int. Conf. on Joints in Aluminium INALCO'98, Cambridge, UK (1998).
6. E. V. Avtokratova, R. R. Il'yasov, M. V. Markushev, *et al*., Perspekt. Mater., No. 15, 9–14 (2013).
7. M. I. Silis, N. V. Makarov, G. V. Shillo, and T. N. Smirnova, Metalloved. Termich. Obrab. Met., No. 4(646), 34–38 (2009).
8. S. Mironov, Y. Motohashi, T. Ito, *et al*., Mater. Trans., **48**, No. 12, 3140–3148 (2007).
9. E. V. Avtokratova, O. E. Mukhametdinova, O. Sh. Sitdikov, *et al*., Lett. Mater., **4**, No. 2, 93 (2014).